ISSN: 2277-3754
ISO 9001:2008 Certified
International Journal of Engineering and Innovative Technology (IJEIT)
Volume 5, Issue 3, September 2015

Impedance and dielectric studies of gel grown lead-iron mixed levo tartrate crystals

H.O. Jethva[*1], M.J. Joshi[1] and D. K. Kanchan[2]
[1]Crystal Growth Laboratory, Department of Physics, Saurashtra University, Rajkot 360 005, India
[2]Solid State Ionics and Glass Research Lab, Department of Physics, Faculty of Science, M S University of Baroda, Vadodara, India

Abstract: ***Various metal tartrate crystals find different applications. In the present study, the lead-iron mixed levo tartrate crystals with different compositions were grown by using silica hydro gels as the growth medium. Long, dendrite, white crystals were grown. From EDAX the exact composition of lead and iron was estimated in the grown crystals. The thermo- gravimetric analysis was carried out to assess the amount of water molecules associated with them. The FTIR spectroscopy study was carried out to identify the presence of various functional groups. The stoichiometric formulae of different composition of mixed Pb- Fe levo tartrate crystals were suggested. The impedance spectroscopic studies were carried out on pelletized samples in 100 Hz to 7 MHz range at room temperature. The variation of the real and imaginary part of impedance was studied with frequency of applied field. From the Nyquist plots and computer simulation of equivalent circuits the contribution of grain and grain boundary was revealed. The variation of dielectric constant and dielectric loss with frequency was also studied. The variation of ac conductivity with frequency has been discussed according to Jonscher's law.***

Keywords. **Gel growth, impedance spectroscopy, dielectric study, ac conductivity, Jonscher's law.**

I. INTRODUCTION

The metal tartrate crystals find various applications, for example, ferroelectric applications of calcium tartrate [1], piezoelectric application of cadmium tartrate [2], iron (III) tartrate acting as a photo activator in light induced oxidative degradation of white wine [3], carbonate solutions containing Co(II) tartrate complexes in an electrochemical procedure of anodic deposition of cobalt oxihydroxide film on a glassy carbon substrate in an alkali medium [4]and lead tartrate as an additive in gasoline to prevent knocking in motors [5]. The growth and characterization of several metal tartrate crystals has been reported, for example, lead tartrate [6,7], iron tartrate [8], mixed iron-manganese tartrate [9], ternary iron-manganese-cobalt tartrate [10], ternary iron-manganese-nickel tartrate compound [11], mixed lead-cadmium levo tartrate [12] and mixed lead-iron levo tartrate crystals [13].

Complex impedance spectroscopy technique is very important tool to investigate the electrical properties of the materials. This technique is able to resolve the contributions of various processes such as electrode effects, bulk effects and the interfaces, viz., the grain boundaries, etc., in the frequency domain. The impedance spectroscopy study has been reported for several types of compounds, for instance, CdS nano particles [14], bismuth layered $SrBi_2Nb_2O_9$ (SBN) perovskite compounds [15], lead-free piezoelectric perovskite ceramic $(Bi_{0.5}Na_{0.5})_{0.95}Ba_{0.05}TiO_3$(BNT-$BT_{0.05}$) [16], CuO nano-grains [17] and doped manganites ($Pr_{0.4}Ca_{0.6}MnO_3$) polycrystalline compounds [18]. Earlier, several authors have reported dielectric studies of several tartrate crystals, viz., Cu^{+2} doped calcium tartrate tetra hydrate crystals [19], zinc tartrate [20] and iron-manganese-cobalt ternary tartrate [10]. However, no major work is reported on impedance spectroscopy in metal tartrate crystals.

Earlier, the present authors have reported the structural, thermal and spectral studies and suggested the stoichiometric formulae of lead –iron mixed levo tartrate crystals [13]. In order to further study the electrical properties of lead-iron mixed levo tartrate crystals, the present authors report the impedance spectroscopy and dielectric study in the present communication.

II. EXPERIMENTAL

In the present study, the single diffusion gel growth technique was employed to grow mixed levotartrate crystals of lead and iron. The gelling solution was obtained by mixing sodium metasilicate solution of specific gravity 1.05 with 1 M levo tartaric acid solution in such a manner that the pH of the mixture was obtained 4.5. This solution was poured in test tubes of 150 mm length and 25 mm diameter to set in the gel form. The following mentioned compositions of supernatant solutions were poured gently on the set gels:

(I) 1 M, 10 ml $Pb(NO_3)_2$

(II) 1 M, 4 ml $Pb(NO_3)_2$ + 1 M, 6 ml $Fe(NO_3)_2$ $9H_2O$

(III) 1 M, 6 ml $Pb(NO_3)_2$ + 1 M, 4 ml $Fe(NO_3)_2$ $9H_2O$

(IV) 1 M, 8 ml $Pb(NO_3)_2$ + 1 M, 2 ml $Fe(NO_3)_2$ $9H_2O$

All the chemicals were of AR grade and obtained from Sigma Aldrich. The following reaction was expected to occur in the formation of lead- iron mixed levo tartrate crystals.

$$(1 - X)Pb(NO_3)_2 + XFe(NO_3)_2{\cdot}9H_2O + H_2C_4H_4O_6 + nH_2O \rightarrow Fe_XPb_{(1-X)}C_4H_4O_6{\cdot}\ nH_2O + 4HNO_3 + 8H_2O + 1/2O_2 \quad (1)$$

Where, the value of X is to be determined from the EDAX analysis exactly. For X=0 gave the pure lead levo tartrate crystals.

ISSN: 2277-3754
ISO 9001:2008 Certified
International Journal of Engineering and Innovative Technology (IJEIT)
Volume 5, Issue 3, September 2015

Figure 1 (a-d) is the photographs of the dendrite type crystals growing inside the test tubes for the supernatant solutions (I-IV), respectively.

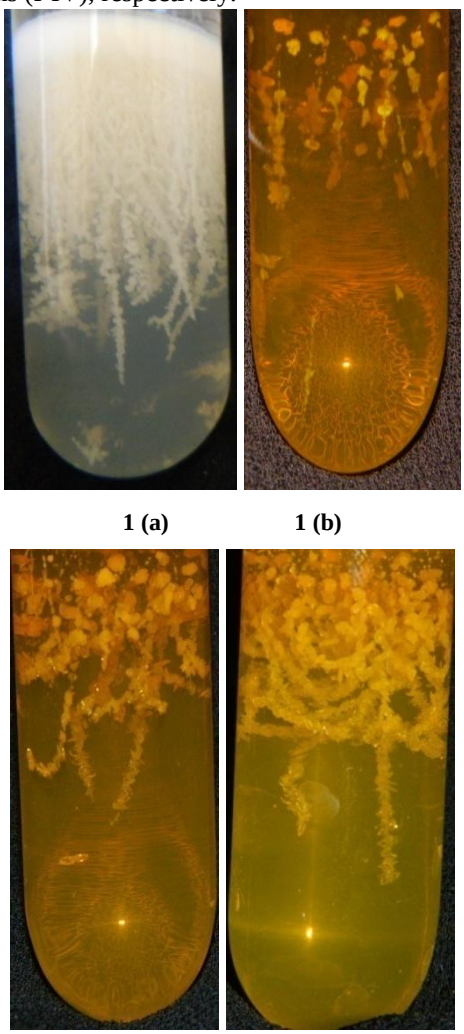

1 (a) **1 (b)**

1 (c) **1 (d)**

Fig 1. Growth of crystals in test tube

III. CHARACTERIZATION TECHNIQUES

The determination of composition of metallic elements in the crystals was carried by the EDAX using Philips Xl – 30 set up. The FTIR spectra were recorded on pelletized samples in KBr media in frequency range of 400 cm $^{-1}$ to 4000 cm $^{-1}$ using Perkin Elmer Spectrum GX instrument. The thermo-gravimetric analysis (TGA) was carried out to assess the presence of water of hydration. TGA was carried out from room temperature of 30^{o}Cat a heating rate of 10^{o}C/min in atmosphere of air using Linseis (STA PT 1600) set up. The synthesized samples were ground to very fine powder and made into pellets without any binder. As the samples are organo-metallic compounds, they may react with the conductive layers of the coating material. Therefore, pellets without any coatings were used for impedance measurements. The density and porosity of the pellets were not measured but the pellets were prepared in the uniform manner by applying a pressure of 5 ton/sq.cm. The real and imaginary parts of complex impedance were measured for the pelletized samples of different compositions of Pb and Fe as a function of frequency ranging from 100 Hz to 7 MHz at room temperature using SI – 1260 Solartron impedance/gain phase analyser. The obtained impedance data were analyzed by the equivalent circuit software Zview available with the instrument SI – 1260 Solartron. Using this software, all the circuit parameters were adjusted simultaneously in order to fit the measured data and to obtain resistances, capacitances, relaxation frequencies and the equivalent circuit of the materials under study. The value of dielectric constant was calculated by using dielectric formulations available in the literature [21].

IV. RESULT AND DISCUSSION

Often many crystals exhibit the dendrite type crystal growth. The mechanism of dendrite crystal growth was studied by Fujiwara and Nakajima [22]. Dendrite type growth morphology has been observed by several authors in the gel grown crystals, such as ammonium tartrate [23], lanthanum tartrate [24], barium oxalate [25], strontium iodate [26], lead tartrate [6] and cadmium tartrate [20].The details of the dendrite type growth is discussed elsewhere [12,13].The composition of grown crystals was determined by EDAX. The stoichiometric formulae were suggested on the basis of EDAX results as $Pb_{0.989}Fe_{0.011}C_4H_4O_6{\cdot}nH_2O$, $Pb_{0.993}Fe_{0.007}C_4H_4O_6{\cdot}nH_2O$ and $Pb_{0.994}Fe_{0.006}C_4H_4O_6{\cdot}nH_2O$ for sample (II-IV) respectively, and that corresponds to our earlier results on lead-iron levo tartrate [13]. It is observed that the percentage weight of iron in the grown crystals is very less than lead, which may be due to higher hydrated radii of Fe^{+2} ions compared to Pb^{+2} ions and dealt with detailed discussion by the present authors elsewhere [13].

The FTIR spectrum of the grown crystals is shown in the figure 2 for the sample (I-II). Almost the similar behavior is observed for the samples (III) and (IV) and discussed in detail elsewhere [13].

Various absorptions bands occurring are assigned as : 3380 cm^{-1} indicates O-H stretching vibrations, 2930 cm^{-1} indicates asymmetrical C-H stretching vibration, 2630 cm^{-1} suggests bonded O-H stretching vibration, 1590 cm^{-1} suggests C=O stretching vibration, 1380 cm^{-1}indicates C-H bending vibration of alkane, 1125 cm^{-1} indicates C-O stretching vibration, 835 cm^{-1} indicates C-C bending vibration and below 700 cm^{-1} suggests metal-oxygen stretching vibrations.

The powder XRD patterns of the grown crystals for the sample (I-II) are shown in the figure 3 and almost the similar patterns were observed for the samples (III) and (IV) [13].

ISSN: 2277-3754
ISO 9001:2008 Certified
International Journal of Engineering and Innovative Technology (IJEIT)
Volume 5, Issue 3, September 2015

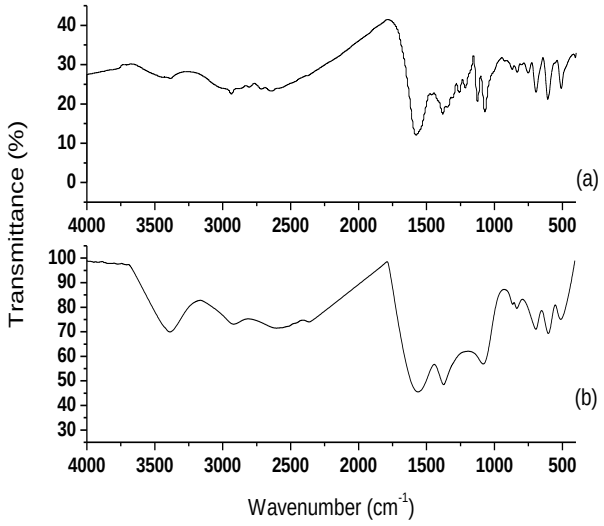

Fig 2. FTIR spectrum of (a) sample (I) and (b) sample (II)

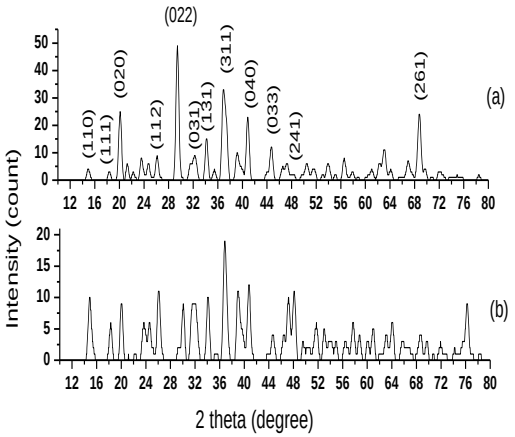

Fig 3. Powder XRD patterns of (a) sample (I) and (b) sample (II)

It was observed that the intensity of all the peaks of mixed Pb-Fe levo tartrate crystalswere reduced with comparison to pure lead tartrate crystals, but there was no significant change in the peak positions in the XRD patterns. No separate phase due to the presence of iron was identified [13]. The orthorhombic unit cell parameters of lead tartrate crystals are : a = 7.99482 Å, b = 8.84525 Å and c = 8.35318 Å with space group $P2_12_12_1$ [27], while the orthorhombic unit cell parameters of iron tartrate crystals are: a = 8.7588 Å, b = 10.9889 Å and c = 8.1900 Å [9]. In the present study, the unit cell parameters of mixed crystals of Pb and Fe levo tartrate are: a = 8.0048 Å, b = 8.8452 Å, c = 8.3532 Å for sample (II), a = 7.9820 Å, b = 8.8400 Å, c = 8.3550 Å for sample (III) and a = 7.9920 Å, b = 8.8500 Å, c = 8.3540 Å for sample (IV), which are found close to the unit cell parameters of pure lead tartrate. This is due to very low content of iron in the mixed crystals of Pb and Fe levo tartrate.

The TG curves of the grown crystals are shown in the figure 4 for the sample (I-II). Almost the similar nature is observed for the samples (III) and (IV).

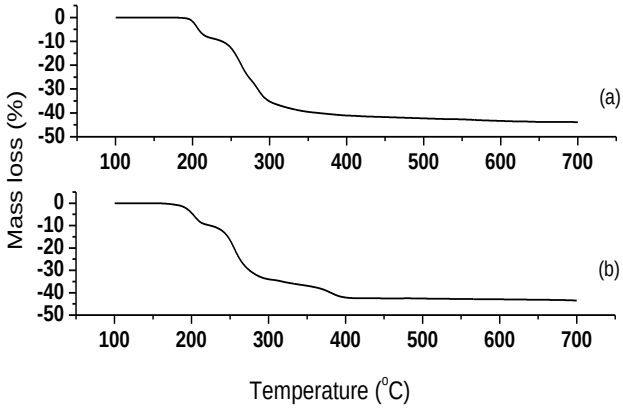

Fig 4. TG plots of (a) sample (I) and (b) sample (II)

No decomposition is observed for the sample (I) from room temperature to 240°C and for the samples (II-IV) from room temperature to 160°C to 170°C. The sample (I) is converted into anhydrous form at temperature 200°C to 240°C, while samples (II-IV) are converted into anhydrous form at temperature 200°C to 210°C. The anhydrous form of sample (I) is converted into carbonate form at temperature 300°C, while samples (II-IV) are converted into carbonate form within temperature 270°C to 280°C. Finally, the carbonate form of sample (I) is converted into oxide form at temperature 600°C, whereas the samples (II-IV) are converted into oxide form at temperature 400°C.The detailed analysis is discussed by the present authors elsewhere [13]. The amount of water molecules attached with the samples (I-IV) have been calculated and given in table 1 with stoichiometric formula.

Table 1. Stoichiometric formula for pure Pb and Pb Fe mixed levo tartrate crystals

Sample name	Estimated formula from EDAX and TGA
Sample (I)	$PbC_4H_4O_6$ $2.4H_2O$
Sample (II)	$Pb_{0.989}Fe_{0.011}C_4H_4O_6$ $1.9H_2O$
Sample (III)	$Pb_{0.993}Fe_{0.007}C_4H_4O_6$ $0.5H_2O$
Sample (IV)	$Pb_{0.994}Fe_{0.006}C_4H_4O_6$ $0.17H_2O$

A. Impedance Studies

The complex impedance plot, called the Nyquist plot, gives one or two semi-circular arcs, depending upon the relative values of their relaxation times. Each of these semicircles could be represented by a single RC combination. The semicircle passes through a maximum at a frequency fr, called the relaxation frequency and satisfies the condition $\omega\tau = 1$. On the other hand, complex modulus or permittivity plane plots are used to represent

ISSN: 2277-3754
ISO 9001:2008 Certified
International Journal of Engineering and Innovative Technology (IJEIT)
Volume 5, Issue 3, September 2015

the response of dielectric systems [28]. Complex impedance plane plots of Z' versus Z'' are useful for determining the bulk resistance of a sample, while the complex modulus plots are useful in determining the smallest capacitance. Sinclair and West [29] suggested the combined usage of impedance and modulus spectroscopic plots to rationalize the dielectric properties. Impedance spectroscopy study of various electro-materials [30], thin films [31], Co-implanted ZnO single crystals [32] and CuO nano-grains [17] has been reported in terms of equivalent circuits and their circuit components contributions.

Figure 5(a) shows the Nyquist diagram (Z'' vs. Z') at room temperature for sample (I), while figure 5(b) shows the same diagram at room temperature for the samples (II-IV). The value of grain resistance (R_g) and corresponding grain capacitance (C_g) as well as grain-boundary resistance (R_{gb}) and corresponding grain-boundary capacitance (C_{gb}) and relaxation frequency were also obtained by the software Z-view when data were simulated by the software Z-view to obtain the best fit equivalent circuit. If these materials have two or more contributions with different relaxation times, then two or more circular arcs are observed in their complex plane impedance (Z'' vs Z') plots [29,33-35].

A closer look of Nyquist plot of figure 5(a) near the origin clearly indicates the steep rising arc and a presence of a one more semi-circle near the origin, which can be viewed in detail manner by using the software Zview in the region near to the origin and shown in the inset of figure 5 (a).

This small semicircle near high frequency is due to grains. The remaining large semicircle at low frequency indicates the grain boundary effect. The intercept of the semicircle on the real axis gives the bulk resistance of grain (R_g) and grain boundary (R_{gb}) of the corresponding component contributing towards the impedance of the sample. This is represented in the form of two parallel RC elements in series as shown in figure 6(a). The two semi-circular arcs in the impedance plane plots show the presence of two relaxation process in the system with different relaxation frequencies.

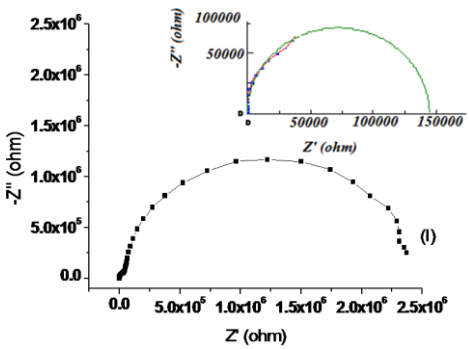

Fig 5(a). Nyquist diagram of sample (I)

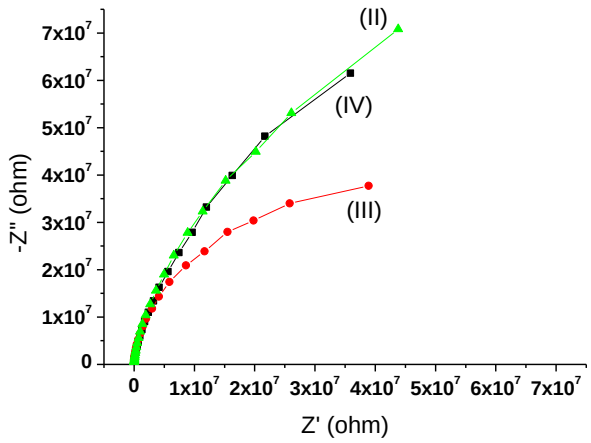

Fig 5(b). Nyquist diagram of sample (II-IV)

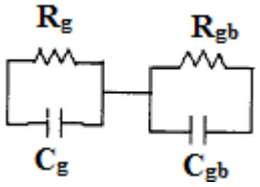

Fig 6(a). Equivalent circuit of sample (I)

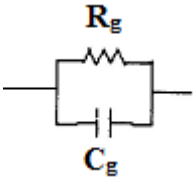

Fig 6(b). Equivalent circuit of samples (II-IV)

As the iron content is added into the pure Pb levo-tartrate sample, only one semi-circular arc appears for all the three samples (II-IV) of Pb-Fe mixed levo-tartrate crystals shown in the Nyquist plot (figure5(b)). Polycrystalline materials are heterogeneous in nature due to effects of grains and grain boundaries in the ac electrical properties [18]. Due to less thickness of grain boundaries compared to grain interiors, grain boundaries offer high resistance. Therefore, larger is the product RC and lower would be the relaxation frequency. A parallel RC combination (Rg, Cg), shown in figure 6(b), was found to have excellent fit with the experimental data, there by indicating the contribution from grains of the samples. The centres of all the three semicircles lie below the real axis having comparatively large radii. The radius of the semicircle indicates the resistivity of the material [16]. There is no systematic change observed in the radii with the composition of the samples, indicating no systematic variation in the resistivity of the samples observed with the composition of the samples due to very low percentage weight (1.1% and less) of iron in the samples.

The values of R_g, R_{gb}, C_g, C_{gb} and relaxation frequency for the pure Pb levo-tartrate crystals of sample (I) and the values of R_g, C_g and relaxation frequency for the mixed

ISSN: 2277-3754
ISO 9001:2008 Certified
International Journal of Engineering and Innovative Technology (IJEIT)
Volume 5, Issue 3, September 2015

Pb-Fe levo-tartrate crystals of samples (II-IV) at room temperature are obtained by using the software and listed in table 2.

Table 2. Grain and grain boundary resistances and capacitances

Sample Name	R_g (MΩ)	R_{gb}(MΩ)	C_g (pF)	C_{gb} (pF)	Relaxation frequency
$PbC_4H_4O_6$ $2.4H_2O$	0.145	2.38	103	66.5	f_g = 10.6 kHz f_{gb} = 1 kHz
$Pb_{0.989}Fe_{0.011}C_4H_4O_6$ $1.9H_2O$	169	--------	16	--------	f_g = 55 Hz
$Pb_{0.993}Fe_{0.007}C_4H_4O_6$ $0.5H_2O$	86.2	--------	7.99	--------	f_g = 229 Hz
$Pb_{0.994}Fe_{0.006}C_4H_4O_6$ $0.17H_2O$	210	--------	9.03	--------	f_g = 82 Hz

The values of grain resistances are higher than that of the pure lead tartrate crystals and indicate the clear effect of presence of iron additive. In the Nyquist curve of pure lead tartrate, the equivalent circuit shows the effect of both grain and grain boundaries, while in the mixed lead-iron levo tartrate the equivalent circuit shows the effect of increasing grain resistances and absence of grain boundary resistances. It is found that the majority amount of iron enters the crystalline lattice due to substitutional nature of iron and the grain resistance changes. There is a marked change in the electrical properties and equivalent circuits found with comparison to pure lead levo tartrate on addition of iron. It is observed from the Table 2 that there is no systematic variation in the values of grain resistances for Pb-Fe mixed levo tartrate.

B. Dielectric Study

Figure 7 and figure 8 show the variation of the real (ε') part and imaginary (ε'') part of dielectric constant with frequency at room temperature for all the four samples (I-IV), respectively.

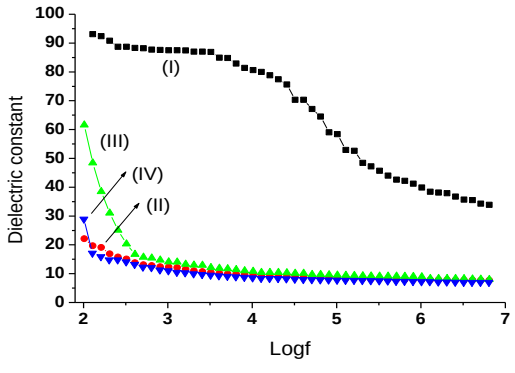

Fig 7. A plot of dielectric constant with frequency

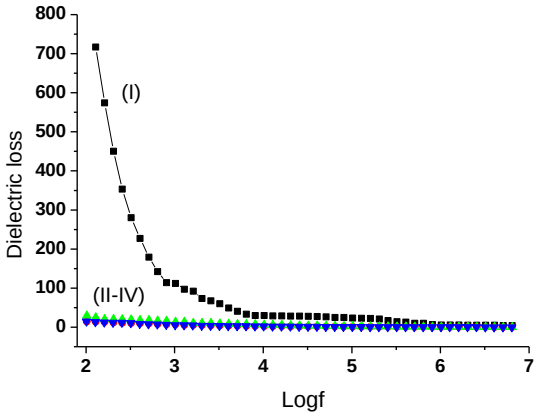

Fig 8. A plot of dielectric loss with frequency

The real part of dielectric constant (ε') and imaginary part of dielectric constant (ε'') is calculated by using the formula given in the equation (2) and (3).

$$\varepsilon' = \frac{t}{\omega A \varepsilon_0} \frac{Z''}{Z'^2 + Z''^2} = \frac{t}{2\pi f A \varepsilon_0} \frac{Z''}{Z^2} \quad (2)$$

$$\varepsilon'' = \frac{t}{2\pi f A \varepsilon_0} \frac{Z'}{Z^2} \quad (3)$$

Where, A = Cross-section area of the pellet, t = Thickness of the pellet, ε0 = Permittivity of free space = 8.854 × 10-12 F/m and Z2 = Z'2 + Z''2.

It is seen that the values of both dielectric constant and dielectric loss decreases with increase in frequency, which is a common feature in many compounds such as iron-nickel-manganese ternary levo-tartrate crystals [11], zinc tartrate [20], 4-(2-hydroxyphenylamino)-pent-3en-2-one (HPAP) [36], and zinc doped nano-hydroxyapatite [37]. Continuous gradual decrease in the values of dielectric constant and dielectric loss suggests that the crystals, like any normal dielectric, may have domains of different sizes and varying relaxation times. The high value of dielectric constant at lower frequencies may be due to the presence of ionic polarizations and/or space charge polarizations. At low frequencies, the dipoles can easily switch their alignments with the changing field. As the frequency increases, both the dielectric constant and dielectric loss values are found constant and attain lower values which indicate that the dipoles do not comply with oscillating electric field. The addition of iron reduces the grain capacitance of Pb levo tartrate in the dielectric measurements, as the capacitance is proportional to the dielectric constant,, which further results in the reduction of dielectric constant of the mixed Pb-Fe levo tartrate crystals. As compared to pure lead levo tartrate crystals, the dielectric loss is very low in lead- iron mixed levo tartrate crystals due to the presence of iron in the

ISSN: 2277-3754
ISO 9001:2008 Certified
International Journal of Engineering and Innovative Technology (IJEIT)
Volume 5, Issue 3, September 2015

structure. It is observed from the figure 7 that the dielectric constant also changes in non-systematic manner for the different composition of iron in the samples (II-IV).

C. Conductivity Analysis

When the conductivity is measured with frequency $\omega = 2\pi\upsilon$ of an alternating electric field, the response of the material whether crystalline or amorphous, can be represented by an equation proposed by Jonscher [38].

$$\sigma_{total} = \sigma_{dc} + A\omega^{n} \quad (4)$$

where, σdc is the direct current or static conductivity at the low frequency where the ion is migrated or diffusion of cation occurs for long distance in the material, Aωn is the ac conductivity due to the dispersion phenomena occurring in the material at higher frequency, A is a temperature dependent constant which determines the strength of polarizibility (or non-ideal conductivity) arising from diffusive motion of carriers [39] and n is a function of temperature as well as frequency, which generally varies between 0 and 1 and represents the interaction between the charge carriers participating in the polarization process [39].

The nature of ac conductivity with frequency of applied field for all the four samples (I-IV) is shown in the figure 9.

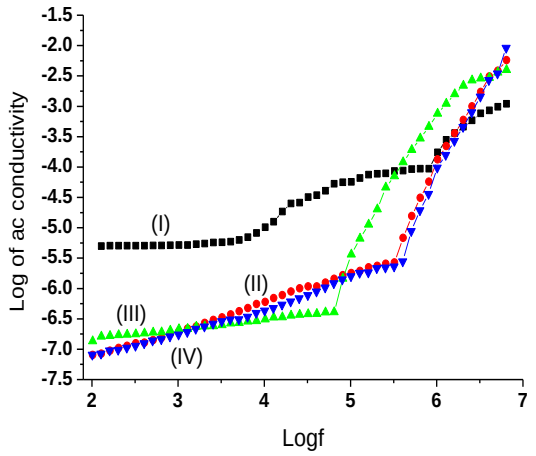

Fig 9. Variation of ac conductivity with frequency

It is observed from the figure that the conductivity increases gradually as frequency increases. The electrode polarization effects are found to cover-up the dc conductivity plateau region and are absent in the dispersive region at high frequencies. The low conductivity value at low frequencies is related to the accumulation of the ions due to the slow periodic reversal of the electric field. In the high frequency or in mid-frequency region, the Jonscher's power law nature is observed and conductivity increases with frequency.

The values of constant A and *n* are listed in the table 3.

Table 3. The values of *n* and *A* for all the samples (I-IV)

Sample	*n*	*A* (S m^{-1})
Sample (I)	0.62	4.38×10^{-8}
Sample (II)	0.90	2.78×10^{-10}
Sample (III)	0.95	2.13×10^{-10}
Sample (IV)	0.88	2.72×10^{-10}

It can be observed form the values of n and A that the degree of interaction of mobile ions with the lattice as well as the strength of polarizability are almost the same for the samples (II-IV), indicating effect of composition is not significant because the variation of Fe in the sample is from 1.1% to 0.6% and gives no major contribution. But in the pure lead levo tartrate sample the value of n is comparatively low and the value of A is comparatively high. The high value of A for pure lead tartrate crystals indicates high strength of polarizability; i.e., the dipoles per unit volume in pure Pb levo-tartrate crystals can align well in the direction of applied varying electric field is higher compared to the mixed Pb-Fe levo-tartrate crystals. The polarizability of an atom or molecule depends on its dimension, as per the simple estimate for spherical atom or molecule the polarizability is proportional to the cube of its radius [40]. The higher value of ionic radius of Pb (1.19Å) compared to Fe (0.55 Å) leads higher polarizability of lead than iron. As the polarizability is related to the dielectric constant by the following relation:

$$\alpha=\varepsilon_0(K-1)/n \quad (5)$$

Where, α= Strength of Polarizability, K= Dielectric Constant, n= Number density

The above equation suggests that higher the value of dielectric constant, the higher is the polarizability. The higher value of polarizability of lead confirms the high value of dielectric constant of pure Pb levo tartrate crystals than mixed Pb-Fe levo tartrate crystals. As iron is added into the pure Pb levo tartrate crystals, the value of A in Jonscher's equation is reduced, indicating low polarizability and dielectric constant [39]. This is in correspondence to the impedance spectroscopy study results.

Want et al [41] suggested the protonic conduction from the variation of ac conductivity in gadolinium tartrate trihydrate crystals with temperature. On the other hand, Arora et.al. [42] Reported that the strontium tartrate trihydrate crystals possessed conductivity between semiconductor and insulator and they further suggested the Efros-Shklovski hopping mechanism for the conduction. Funke [43] explained the physical significance of *n* in Jonscher's equation in two different regimes, i.e., $n \leq 1$ would indicate that the sudden hopping motion is due to translational motion and the value of $n > 1$ would mean that the motion is a localized hopping of the species with a small hopping without

ISSN: 2277-3754
ISO 9001:2008 Certified
International Journal of Engineering and Innovative Technology (IJEIT)
Volume 5, Issue 3, September 2015

leaving the neighborhood [44]. Usually, in case of ionic conductors, the value of *n* can lie between 1 and 0.5 indicating the ideal long range pathways and diffusion limited hopping (tortuous pathways) [45]. Moreover, the Jump Relaxation Model (JRM) developed by Funke and Riess [46] attributes the dispersion in the conductivity to strong forward-backward jump correlations in the motion of ions. According to this model, after a hop of a central ion from initially relaxed local configurations, it is no longer in equilibrium with its surroundings. In order to stabilize the new position of the ion, the other ions and their environments have to move. On the other hand, the ion can also jump back in order to partially relax the configuration after the jump. The longer the ion stays at the new position after the jump, the lesser the preference to jump backward.

The variation of dielectric constant is within the values of 93 to 34 for sample (I), 22 to 7.7 for sample (II), 61 to 8 for sample (III) and 28 to 6.7 for sample (IV) between the frequency range 100 Hz to 7 MHz. Singh and Ulrich [47] classified various dielectric materials according to the values of dielectric constant, that is, the high dielectric materials have k > 7 and the low dielectric materials having k <3.9. Comparing the dielectric results with this classification, the present samples possess high values of dielectric constant and they may find the application mainly in three areas such as memory cell dielectrics, gate dielectrics and passive components after complete electrical and physical characterizations.

V. CONCLUSION

The pure lead levo tartrate and lead-iron mixed levo-tartrate crystals were grown in silica gel by varying the volume of lead nitrate and iron nitrate in supernatant solutions. The lower percentage of iron in the crystalline lattice was explained on the basis of hydrated radii of lead and iron. The lead –iron mixed levo tartrate crystals, exhibited only one semi-circle indicating the presence of grain effects whereas pure lead levo tartrate exhibited two semi-circles indicating the effects of both grain and grain-boundary.

In comparison to pure lead levo tartrate, the low values of dielectric constant and dielectric loss for lead-iron levo tartrate crystals were due to the presence of iron at grain position. The ac conductivity variation with frequency obeys the Jonscher's power law. The ac conductivity in the present system is considered due to the hopping motion with the ideal long range and diffusion limited pathways. Lead-iron mixed levo tartrate crystals exhibited remarkable change in electrical parameters in comparison to pure lead tartarte.

ACKNOWLEDGEMENT

The authors are thankful to the HOD Physics (Saurashtra University, Rajkot and M. S. University, Vadodara) for their kind co-operation. The author (HOJ) is thankful to the Principal and Management of Maharaja Shree Mahendrasinhji Science College, Morbi, Gujarat, India for the encouragement.

REFERENCES

[1] H. B. Gon, J. Cryst. Growth. 102, 501 (1990).

[2] J. S. Hopwood and A. W. Nicol, Crystallogr. J. Online. 1600, 5767 (1972).

[3] A. C. Clark, D. A. Dias, T. A. Smith, K. P. Ghiggino and G. R. Scollary, J. Agric. Food. Chem. 59(8), 3575 (2011).

[4] I. G. Casella, J. Electroanal. Chem. 520(1-2), 119 (2002).

[5] N. J. Rahway, The Merck Index of Chemicals and Drugs. 6th ed., Merck & Co., USA, (1952).

[6] M. Abdulkadhar and M. A. Ittyachen, J. Cryst. Growth. 39, 365 (1977).

[7] H. O.Jethva and M. V. Parsania, Asian J. Chem. 22(8), 6317 (2010).

[8] S. Joseph, H. S. Joshi and M. J. Joshi, Cryst. Res. Technol. 32(2), 339 (1977).

[9] S. J. Joshi, B. B. Parekh, K. D. Parikh, K. D. Vora and M. J. Joshi, Bull. Mater. Sci. 29(3), 307 (2006).

[10] S. J. Joshi, K. P. Tank, B. B. Parekh and M. J. Joshi, Cryst. Res. Technol. 45, 303 (2010).

[11] S. J. Joshi, K. P. Tank, B. B. Parekh and M. J. Joshi, J. Therm. Anal. Calorim. 112, 761 (2013).

[12] H. O. Jethva, P. M. Vyas, K. P. Tank and M. J. Joshi, J. Therm. Anal. Calorim. 117(2), 589 (2014).

[13] H. O. Jethva and M. J. Joshi, Int. J. Eng. Innov. Technol. 4(1), 121 (2014).

[14] R. Triphathi, A. Kumar and T. P. Sinha, Pramana J. Phys. 72(6), 969 (2009).

[15] M. P. Dasari, K. SambasivaRao, P. Murali Krishna and G. Gopala Krishna, Acta. Physica. Polonica. A 119, 387 (2011).

[16] A. K. Roy, K. Prasad and A. Prasad, Process. Appl. of Ceramics. 7(2), 81 (2013).

[17] M. Younas, M. Nadeem, M. Idrees and M. J. Akhtar, Appl. Phys. Lett. 100, 152103(1-4) (2012).

[18] M. Shah, M. Nadeem, M. Idress, M. Atif and M. J. Akhtar, J. Magn. Magn. Mater. 332, 61 (2013).

[19] S. R. Suthar, S. J. Joshi, B. B. Parekh and M. J. Joshi, Indian J. Pure & Appl. Phys. 45, 48 (2007).

[20] R. M. Dabhi, B. B. Parekh and M. J. Joshi, Indian J. Phys. 79(5), 503 (2005).

[21] D. K. Pradhan, R. N. P. Choudhary and B. K. Samantaray, Int. J. Electrochem. Sci. 3, 597 (2008).

[22] K. Fujiwara and K. Nakajima, Mechanism of dendritic crystal growth. Springer, (2009).

[23] A. D. Saraf, K. B. Saraf, P. A. Wani and S. V. Bhoraskar, Cryst. Res. Technol. 21(4), 449 (1986).

[24] P. N. Kotru, N. K. Gupta and K. K. Raina, J. Mater. Sci. 21, 90 (1986).

[25] P. V. Dalal and K. B. Saraf, Bull. Mater. Sci. 29, 412 (2006).

ISSN: 2277-3754
ISO 9001:2008 Certified
International Journal of Engineering and Innovative Technology (IJEIT)
Volume 5, Issue 3, September 2015

[26] S. J. Nandre, R. R. Ahire and S. J. Shitole, Adv. in Appl. Sci. Res. 2, 134 (2011).

[27] D. J. A. De Ridder, K. Goubitz, E. J. Sonneveld, W. Molleman and H. Schenk, Cryst. Struct. Commun. C58, m596 (2002).

[28] S. P. S. Badwal, Proceedings of the International seminar on Solid State Ionic Devices. Singapore, 165 (1988).

[29] D. C. Sinclair and A. R. West, J. Appl. Phys. 66(8), 3850 (1989).

[30] D. C. Sinclair, Boi. Soc. Esp. Ceram. Vidrio. 34(2), 55 (1995).

[31] J. L. Hertz, A. Bieberle and H. L. Tuller, MIT-Tohoku "21 COE" Joint workshop on nano-science in energy technology, O-11-1, (2004).

[32] M. Younas, L. L. Zou, M. Nadeem, Naeem-ur-Rehman, S. C. Su, Z. L. Wang, W. Anwand, A. Wagner, J. H. Hao, C. W. Leung, R. Lortz and F. C. C. Ling, Phys. Chem. Chem. Phys. 16, 16030 (2014).

[33] J. R. MacDonald, Impedance Spectroscopy, Wiley, New York, (1987).

[34] D. C. Sinclair and A. R. West, J. Mat. Sci. Lett. 7, 823 (1988).

[35] F. D. Morrison, D. C. Sincalir and A. R. West, J. Appl. Phys. 86, 6355 (1999).

[36] B. B. Parekh, D. H. Purohit, P. Sagayaraj, H. S. Joshi and M. J. Joshi, Cryst. Res. Technol. 42, 407 (2007).

[37] K. P. Tank, P. Sharma, D. K. Kanchan and M. J. Joshi, Cryst. Res. Technol. 46, 1309 (2011).

[38] A. K. Jonscher, Dielectric Relaxation in Solids. Chelsea Dielectric Press, London, (1983).

[39] D. Shamiryan, T. Abell, F. Iacopi and K. Maex, Materials today, 7(1), 34 (2004).

[40] R. Murugeshan, Electricity and magnetism, 7th ed., S. Chand, New Delhi (2008) p. 300.

[41] B. Want, A. Farooq and P. N. Kotru, Mater. Sci. & Engineering. 38, 270 (2007).

[42] S. K. Arora, V. Patel, R. G. Patel, B. Amin and A. Kothari, J. of Phys. Chem. and Chem. of Solids. 65, 465 (2004).

[43] K. Funke, Prog. Solid State Chem. 22, 111 (1993).

[44] S. Sen and R. N. P. Choudhary, Mater. Chem. Phys. 87, 256 (2004).

[45] K. A. Mauritz, Macromolecules. 22, 4483 (1989).

[46] K. Funke and I. Riess, Z. Phys. Chem. Neue Folge. 140, 217 (1984).

[47] R Singh and R K Ulrich High and low dielectric constant materials: Materials science Processing and Reliability Issues, 4th Symposium, The Electrochemical Society Interface, Summer 26 (1999).